1-1-2016

# Severity of Spinal Cord Injury Influences Diffusion Tensor Imaging of the Brain

Michael B. Jirjis
*Marquette University*

Aditya Vedantam
*Medical College of Wisconsin*

Matthew D. Budde
*Medical College of Wisconsin*

Benjamin Kalinosky
*Marquette University*, benjamin.kalinosky@marquette.edu

Shekar N. Kurpad
*Medical College of Wisconsin*

Accepted version. *Journal of Magnetic Resonance Imaging*, Vol. 43, No. 1 (January 2016): 63-74. DOI.

# Severity of Spinal Cord Injury Influences Diffusion Tensor Imaging of the Brain

Michael B. Jirjis
*Department of Biomedical Engineering, Marquette University, Milwaukee, WI*
Aditya Vedantam
*Department of Neurosurgery, Medical College of Wisconsin, Milwaukee, WI*
Matthew D. Budde
*Department of Neurosurgery, Medical College of Wisconsin, Milwaukee, WI*
Benjamin Kalinosky
*Department of Biomedical Engineering, Marquette University, Milwaukee, WI*
Shekar N. Kurpad
*Department of Neurosurgery, Medical College of Wisconsin, Milwaukee, WI*

*Journal of Magnetic Resonance Imaging*, Vol 43, No. 1 (January 2016): pg. 63-74. DOI. 

Brian D. Schmit

*Department of Biomedical Engineering, Marquette University, Milwaukee, WI*

**Abstract**

**Background:** The purpose of this study was to determine whether DTI changes in the brain induced by a thoracic spinal cord injury are sensitive to varying severity of spinal contusion in rats.

**Methods:** A control, mild, moderate, or severe contusion injury was administered over the eighth thoracic vertebral level in 32 Sprague-Dawley rats. At 11 weeks postinjury, ex vivo DTI of the brain was performed on a 9.4T Bruker scanner using a pulsed gradient spin-echo sequence.

**Results:** Mean water diffusion in the internal capsule regions of the brain and pyramid locations of the brainstem were correlated with motor function ($r^2 = 0.55$). Additionally, there were significant differences between injury severity groups for mean diffusivity and fractional anisotropy at regions associated with the corticospinal tract ($P = 0.05$).

**Conclusion:** These results indicate that DTI is sensitive to changes in brain tissue as a consequence of thoracic SCI.

Monitoring changes in brain structure after spinal cord injury (SCI) could provide important insight into brain reorganization associated with the injury. A useful technique for monitoring brain structure is magnetic resonance diffusion tensor imaging (DTI). DTI parameters reflect spatial patterns of water diffusion and are impacted by membrane barriers associated with cellular structure of the nervous system.[1,2] Changes in DTI parameters of the brain after spinal injury are expected because Wallerian degeneration of spinal tracts, changes in synaptic connections and cellular reactions associated with a spinal injury are expected to alter cellular structure in the brain. In fact, DTI changes have been documented in the brain after spinal cord injury in both rats and humans, with significant differences occurring in the thalamus, corticospinal tract, primary somatosensory cortex, corona radiate, and internal capsule regions.[3-6] Although SCI produces changes in brain diffusion metrics, the effects of specific characteristics of the spinal injury on brain DTI are unknown. The purpose of the current study was to determine whether DTI changes in the brain are sensitive to severity of spinal injury. Specifically, a chronic contusion injury in rats, with ex vivo brain DTI brain imaging was used to test

*Journal of Magnetic Resonance Imaging*, Vol 43, No. 1 (January 2016): pg. 63-74. DOI. 

the hypothesis that DTI parameters of the brain are sensitive to severity of SCI.

# Material and Methods

## *Animals and Spinal Cord Injury Procedure*

All experimental procedures were approved by the Institutional Animal Care and Use Committees (IACUC) at Marquette University, the Medical College of Wisconsin, and the Zablocki VA Medical Center.

Rats were anesthetized with a 0.890 mL/kg of body weight intraperitoneal (IP) dose of 40 µL xylazine, 0.1 mL of acepromazine, and 0.75 µL of ketamine hydrochloride diluted 1:1 with deionized water. Additional half doses were given based on leg flexion-withdrawal and cornea reflexes. Laminectomies were performed for 32 adult female Sprague-Dawley rats weighing between 200 and 250 grams. A weight-drop (10 gram rod) contusion injury was delivered from a height of 0 mm, 10 mm, 25 mm, or 50 mm to produce a control, mild, moderate, or severe injury, respectively, using a MASCIS impactor (W.M. Keck Center for Collaborative Neuroscience; Piscataway, NJ).

Following surgery, rats were placed on a bi-daily postoperative care procedure involving bladder expression, one dose of enrofloxacin (10 mg/kg subcutaneously; Bayer Healthcare LLC; Shawnee Mission, KS), buprenorphine hydrochloride (0.1–0.5 mg/kg subcutaneously; Rickitt Benckiser Health Care Ltd; Hull, UK), and 6 cc of lactated Ringer's solution. Animals were kept under postoperative care procedures until manual bladder expression was no longer needed and signs of stress or infection were no longer present.

## *Behavioral Assessment*

Hindlimb function was assessed on a weekly basis and at 10 weeks after injury using the open field walking procedure outlined by Basso, Beattie, and Bresnahan (BBB).[7] The BBB score is a behavioral assessment of function that looks at open field locomotion and has been strongly related to severity of spinal cord injury in rodents.

Briefly, rats were observed for 3 min on a flat, 1 m diameter surface. BBB scoring was determined by two independently blinded observers, where 0 is flaccid paralysis and 21 is normal gait.

## *Ex Vivo MRI Protocol*

Specimen brains were excised 11 weeks after injury and prepared for ex vivo imaging. The 11 week time point was selected to coincide with a prior study examining DTI parameter changes throughout the spinal cord.[8] Animals were euthanized with an IP injection of sodium pentobarbital (100 mg/kg body weight) and perfused through the heart with 300 mL of saline buffer followed by 600 mL of 10% formalin. The brains were excised and postfixed in a 10% formalin solution until the day of scanning. The brains were immersed in a susceptibility-matching fluid (Fomblin; Solvay Solexis, Inc, West Deptford, NJ) and placed in an inductively coupled 20 mm diameter loop gap radiofrequency coil. Specimens were positioned in a 9.4T Bruker BioSpec 94/30 USR Spectroscopy Imaging System (Bruker BioSpin; Billerica, MA). A multi-echo (eight echos) spin-echo sequence was used to acquire 12 diffusion weighted images (DWIs) with a b-value of 2000 s/mm$^2$ and two images with a b-value of 0 s/mm$^2$. A b-value of 2000 s/mm$^2$ was used for high diffusion contrast. An echo time (TE) of 25 ms and a repetition time (TR) of 3000 ms was used when acquiring scans that had a field of view (FOV) size of 20 mm by 20 mm, acquisition matrix of 128 × 128, and 0.75-mm-thick slices that were contiguously arranged for 30 slices.

## *DTI Analysis*

Diffusion MRI data were imported into the Analysis of Functional NeuroImages software package (AFNI; available at http://afni.nimh.nih.gov/) and co-registered using an iterative least squares fit to the T2-weighted images to correct for eddy-current and susceptibility distortions. There were no slices that were visually affected by eddy-current distortions. Following distortion correction, the resulting matrix volume data were registered to a reference control following the deformable registration approach for tensor-based registration within DTI-ToolKit (DTI-TK) by Zhang et al.[9] The DTI-TK algorithms use a Gaussian smoothing kernel during registration

*Journal of Magnetic Resonance Imaging*, Vol 43, No. 1 (January 2016): pg. 63-74. DOI. 

process; no further smoothing was conducted on the images. Registered tensor volumes were then re-imported into AFNI and the eigenvalues were used to calculate the mean diffusivity (MD; mean of all three eigenvalues), fractional anisotropy (FA; calculated using the formula prescribed by Basser and Pierpaoli[1]), axial diffusivity (LD; primary eigenvalue), and radial diffusivity (RD; mean of the second and third eigenvalues). Registration was visually inspected for alignment at each slice and brains that did not align were removed. Diffusion MRI data were collected and processed before statistical analysis, without knowledge of individual rat severity.

The resulting groups were as follows: Control (n = 8), Severe, (n = 8), Moderate (n = 8), and Mild (n = 8). Eight samples were removed from the study because they exhibited one to two slices that were affected by movement or poor scanning quality. A voxel-wise statistical analysis was completed for both FA and MD diffusion volumes. Manual region of interest (ROI) drawings were also completed before deformable registration of the internal capsule (IC) in the brain as well as corticospinal tract locations in the brainstem for FA, MD, LD, and RD. This was completed to verify that registration differences between specimens did not influence the results. The voxel wise analysis of the brainstem was conducted to determine whether differences would localize to spinal tracts and to verify that results were not limited to cortical and subcortical areas.

## *Immunohistochemistry*

Immunohistochemistry was conducted on two samples from each group to visualize and verify histological changes in the brain that have been reported in literature.[3,10,11] Using an anatomical rat brain atlas, we cut the brain to include two regions of interest: internal capsule and medullary pyramids. Tissue was embedded with paraffin and cut into 20-micron sections using a microtome. Histological sections that matched regions of interest on DTI maps were deparaffinized and rehydrated. Antigen retrieval was performed by microwave heating the slides for 5 min in sodium citrate buffer. Sections were then blocked with blocking buffer (SuperBlock, Thermoscientific, Rockford, IL) for 5 min and incubated overnight with primary antibodies against glial fibrillary acidic protein (1:250,

monoclonal GFAP, MAB360, Millipore, Billerica, MA). After washing with 1× PBS, sections were incubated with goat anti-mouse conjugated Texas Red antibodies (1:250, monoclonal, Jackson ImmunoResearch, West Grove, PA) for 30 min. The sections were then washed, incubated with nuclear stain, DAPI (4',6-diamidine-2-phenylidole-dihydrochloride; 1:500, Sigma-Aldrich, St. Louis, MO) for 10 min and washed again. Finally, Sudan Black stain was added for 1 min to reduce auto-fluorescence. The slides were washed and coverslipped with FluorSave (EMD Millipore Corp., Billerica, MA). Fluorescent images of the internal capsule and medullary pyramids were acquired at 20× magnification using a Nikon Eclipse E600 microscope with Nikon NIS-Elements 4.0 software (Nikon Instruments Inc., Melville, NY).

## *Luxol Fast Blue*

Sections were stained with Luxol fast blue using the method described by Kluver and Barrera.[12] Cresyl violet counterstaining was not performed. Representative images were acquired using an inverted Nikon TE2000-U microscope equipped with a color digital camera at 20× (Nikon Instruments Inc.).

## *Statistical Analysis*

Statistical analysis was carried out using AFNI and the Statistical Package for Social Sciences (SPSS version 13.0; SPSS Inc., Chicago, IL). The distribution of the data was explored using a Shapiro-Wilks test for normality. A one-way analysis of variance (ANOVA) was performed on the DTI images on a voxel by voxel basis to observe statistical variations across groups (fixed factor: injury group; random factor: specimen). To prevent higher frequency components of the images from being recognized as significantly changed clusters,[13] AFNI was used to estimate how spatially smooth the data were. Cluster size was set from this estimation. AFNI's implementation of the false discovery rate algorithm was used to threshold the voxel-wise statistics. Cluster threshold was completed for $F > 4.35$ and $F > 8.45$. After smoothness estimations and statistical analysis thresholding, it was determined that significant clusters needed to connect more than 100 voxels.

*Journal of Magnetic Resonance Imaging*, Vol 43, No. 1 (January 2016): pg. 63-74. DOI. 

A student's t-test was also completed comparing each severity group and $P < 0.05$ was considered to be statistically significant. Mean diffusion values were overlaid onto voxels that were found to be significantly different. For each comparison, the number of voxels that were significant was compared with regions of slice that were not significant. Slices showing significant differences between severity group and control group were overlaid on top of atlas maps,[14] and the number of significant voxels that were located in either the pyramids or the internal capsule was compared with the total number of voxels contained in those specific structures. This was completed to determine volume of significant differences found in those structures for each severity group. For this procedure, a basic rigid-registration was done in Matlab, and comparisons were made for mildly, moderatey, and severely injured rats using Image J 1.46r (National Institutes of Health, Bethesda, MD). A correlation between injury group and BBB score was also conducted using the Spearman correlation on a voxel-by-voxel basis and thresholded for $r^2 > 0.55$. An $r^2$ value of 0.55 was chosen for the threshold for a "large" correlation as outlined by Cohen in 1988.[15] Correlation coefficients at each voxel location were correlated with combined right and left hindlimb scores for each rat.

# Results

## *Functional Motor Assessment*

Hindlimb motor scores, collected at 1 day postinjury and 10 weeks postinjury, are shown in Table 1. These values were within their expected ranges for the targeted injury severity.[7]

## *Diffusion Tensor Imaging of the Brain*

Differences in MD and FA between injury groups were observed in localized regions of the brain. Figure 1 shows the slice locations used for the diffusion tensor imaging results from the rat brain and brainstem. A typical RGB map of a coronal section for a control brain at the level 3.0 mm posterior to the bregma is shown in Figure 2a. A one-way ANOVA revealed significant differences in injury severity groups for the MD and FA at regions consistent with the internal

capsule and thalamus, denoted by voxels in green in Figures 2b (MD) and 2c (FA) ($P < 0.05$). Compared with MD, there appeared to be a higher number of significant regions in the cortex and the midbrain for FA, as seen by visual comparison of Figures 2b and 2c.

Comparisons between injury groups and controls indicated significant localized differences in DTI parameters. T-test comparisons of MD and FA between the control brain and the mild, moderate, and severe brains are shown in Figures 3 and 4. In general, the internal capsule regions of the brain demonstrated significant voxel clusters ($P = 0.039$) in all three SCI groups. The measured FA values in regions corresponding to the internal capsule also showed significant bilateral changes for the injured groups compared with the control ($P = 0.042$).

Our correlation analysis indicated that DTI parameters from specific regions of the brain were correlated with BBB scores. Rat MD voxels with a threshold correlation above $r^2 = 0.55$ ($P = 0.014$) are highlighted in Figure 2d; these highlighted voxels were localized to regions of the internal capsule in the midbrain as well as regions extending out into the cortex (Fig. 2d). The correlation between FA and BBB did not result in large clusters around the internal capsule at the $r^2 = 0.55$ level; however, clusters were visible at $r^2 > 0.40$ (not shown). Although monotonic, the data were nonnormal ($P = 0.044$). In general, when comparing correlation levels, MD still provided reasonable assessment at $r^2 < 0.82$, while FA, RD, and LD appeared to provide reasonable assessment values at $r^2 < 0.60$, $r^2 < 0.63$, and $r^2 < 0.75$, respectively.

## *Diffusion Tensor Imaging of the Brainstem*

Differences in DTI parameters were also observed in localized regions of the brainstem. The mean diffusivity and fractional anisotropy t-maps indicated significant differences between the control group and the injury groups at regions localized to the corticospinal tract, as demonstrated by the color labeled voxels, representing $P < 0.05$, in Figures 5 and 6.

*Journal of Magnetic Resonance Imaging*, Vol 43, No. 1 (January 2016): pg. 63-74. DOI. 

## *Changes in DTI Parameters of the Brain With SCI*

The MD of targeted regions of the brain differed between injury and controls. The relative area of significant difference in MD is shown in Figure 7a for the brain and brainstem slices used in the study. The relative area of significant difference varied by injury severity in both the brain and brainstem. Mild injuries resulted in significant differences ($P < 0.05$) in 9.11% of the brain when compared with the control group. Moderate and severe rats demonstrated an average area of significant difference in MD of 18.28% and 27.79% of the brain. Average percent area of significant differences for mild, moderate, and severe rats in the brainstem was 3.98%, 9.00%, and 23.13%, respectively. Similarly, the percent area that was significantly different from controls within the internal capsule or corticospinal tract also increased with increasing severity of injury (Fig. 7b). Rats that received a mild injury had significant differences ($P < 0.05$) in MD in 76.65% of the internal capsule when compared with controls. Moderately and severely injured rats demonstrated significantly different ($P < 0.05$) areas of 89.88% and 96.07% of the internal capsule compared with the control group. The brainstem spinal tract areas for mild, moderate, and severe groups demonstrated an average percent difference of 50.03%, 67.42%, and 84.75% when compared with the control group.

The differences between severity groups for MD and FA, as well as radial (RD) and axial diffusivities (LD), are demonstrated in Figure 8. MD in the control was significantly greater than the mild ($P = 0.039$), moderate ($P = 0.035$), and severe ($P = 0.002$) internal capsule regions in the brain and corticospinal tract region in the brainstem ($P = 0.046$, $P = 0.045$, and $P = 0.009$, respectively). FA of the control brain was significantly lower than the mild, moderate, and severe brains ($P = 0.035$, 0.040, and $P = 0.0007$, respectively) but not of the corticospinal tract in the brainstem regions. RD of the control brain was significantly higher than the mild, moderate, and severe brains ($P = 0.041$, $P = 0.043$, $P = 0.022$), and LD of the control brain was significantly higher than the mild, moderate, and severe brains ($P = 0.040$, $P = 0.038$, $P = 0.037$). The variability in the brainstem for RD and LD was high and while the control brainstems had higher values, the differences were not significant ($P > 0.05$).

### *Manual Region of Interest Analysis*

The manual ROI analysis confirmed the voxel-wise results. Manual ROIs of the internal capsule and the corticospinal tract in the brainstem were completed before group registration. The MD of the internal capsule regions of the control group was $1.131 \times 10^{-3}$ $mm^2/s$, consistent with the voxel-wise statistical results. The MD values for the internal capsule regions of the injured groups were $1.090 \times 10^{-3}$ $mm^2/s$, $1.074 \times 10^{-3}$ $mm^2/s$, and $1.076 \times 10^{-3}$ $mm^2/s$ for mildly, moderately, and severely injured spinal cords. There was also an increasing trend in FA, as injury severity increased, that matched the voxel-wise statistical analysis. The control group's average FA was 0.304 while the mild, moderate, and severe groups were 0.348, 0.352, and 0.395, respectively. MD and FA ROIs that encompassed the entire control brain were not significantly different than the severity groups ($P > 0.05$).

### *Immunohistochemistry*

Immunohistochemistry indicated changes in brain histology consistent with prior descriptions following chronic SCI.[3,10,11,16] Overall, LFB staining intensity was lower (Fig. 9) and GFAP was more prevalent (Fig. 10) in injured animals. Furthermore, LFB staining intensity of the internal capsule and pyramidal tracts decreased as severity increased while GFAP depicted a larger response in astrocytic immunoreactivity with respect to injury severity (Figs. 9 and 10, respectively). Of particular note, severely injured animals expressed more GFAP compared with the control brain in the internal capsule region. Mild and moderate GFAP expression was not as drastic as the severe rats for the pyramidal tracts and internal capsule.

## Discussion

The results from this study indicate that diffusion tensor imaging in the brain is sensitive to the extent of functional recovery following a spinal cord injury. Our results indicated significant changes in diffusion throughout the brain in injured rats compared with controls, but with greater changes localized to the internal capsule and spinal tracts of the brainstem. The number of significantly changed voxel groups

*Journal of Magnetic Resonance Imaging*, Vol 43, No. 1 (January 2016): pg. 63-74. DOI. 

depended on injury severity, and were correlated with the BBB functional scale. In general, this study documented changes in diffusivity that extended from the spinal cord, through the brainstem and into the brain. Diffusion indices were correlated with a decrease in motor function associated with injury severity.

Recently, other groups have documented changes in DTI parameters in brain structure following SCI. Changes in DTI parameters appear to reflect the tissue microstructural changes that occur after SCI; however, there have been some inconsistencies in the measurements. For example, both Ramu et al and Freund et al report unilateral changes in DTI parameters in the internal capsule region when bilateral differences would be expected, because subjects demonstrated diminished functional outcome for both the left and right limbs.[3,6] Thus, while there is an opportunity to use DTI to assess brain structural changes following SCI, an improved understanding of the changes in brain DTI associated with spinal injury is still needed.

Changes in DTI parameters of the brain after spinal injury are likely due to degeneration of spinal tracts and connected brain regions. The degeneration of spinal white matter tracts extend well beyond the injury zone for up to 1 year after SCI.[19] Recently, we have found that there are systemic changes in DTI parameters that occur along the entire length of the spinal cord following an SCI,[20] and that DTI parameter changes correlate to severity of injury up to 10 weeks.[8] Ten weeks has also been used as a time point by other groups.[18,21] At 10 weeks, the initial acute and inflammatory responses have passed; however, inflammatory cells have been found at locations away from the injury site[22-25] into regions as far from the injury as the brain.[26] These changes appear to accompany the progression of axonal degeneration and likely reflect the underlying structural changes in tissue associated with the histopathological processes that occur after SCI. It is possible that Wallerian degeneration alters membrane structures of the brain and that relative changes in intracellular and extracellular water compartments associated with edema may contribute to changes in diffusion.[8]

Our study demonstrated a decrease in the diffusion of water in regions of the brainstem associated with the corticospinal tract along with a corresponding increase in the fractional anisotropy. These

*Journal of Magnetic Resonance Imaging*, Vol 43, No. 1 (January 2016): pg. 63-74. DOI. 

observations are consistent with an extension of diffusivity changes from the spinal cord into the white matter tracts of the brainstem and brain. We have previously observed decreases in MD in the cervical spinal cord of thoracic injured rats.[20] These data from the rat spinal cord are consistent with observed decreases in MD of the high cervical spinal cord in humans with chronic injuries to lower spinal segments.[27] In the current study, changes in MD and FA at the brainstem level were largely localized to the spinal tract regions, suggesting that diffusivity changes in the brainstem might be linked to degenerating spinal tracts. This localized response in the brain stem differs slightly from observations in the cervical spinal cord in which the entire cross-section of the spinal cord is involved.[8] The percentage of the localized areas that demonstrated significant differences was substantially higher in the internal capsule and corticospinal tract than in the surrounding areas, consistent with a localization of changes to these regions. These differences might be related to differences in the relative portion of tissues within the spinal cord, in which degenerating tracts likely impact most of the spinal cord, compared with brain, which would involve a relatively smaller percentage of tissue.

The localization of changes to spinal tracts within the brainstem suggests that the mechanisms underlying MD decreases in the spinal cord might be related to degenerative processes, rather than a systemic effect throughout the entire central nervous system. Furthermore, the dependence on the severity of injury could reflect a difference in the number of degenerating tracts. RD and LD were calculated to differentiate potential demyelinating and axonal degeneration processes, respectively. Decreases in LD have been associated with axonal degeneration,[28-30] with an asymmetry in rostral caudal directions that is consistent with Wallerian degeneration.[28, 31] The decrease in LD in the brainstem and internal capsule in the current study is consistent with axonal degeneration, but follow-up studies with neurofilament staining are needed to confirm extension of axonal degeneration into the brain. RD decreased in the current study, suggesting that either there was not significant demyelination (indicated by an increase in RD)[32, 33] or that another histopathological mechanism had an impact on water diffusion. The decrease in RD could be interpreted to indicate that an increase in cellularity associated with axonal degeneration had occurred, which would

decrease overall diffusivity and mask an increase in RD associated with demyelination.

The diffusion changes were not limited to just the brainstem, but extended further into the brain as well. We observed a difference between groups for both MD and FA in the internal capsule. These results for MD and FA suggest a possible degeneration of spinal tracts through the brain. The changes in diffusion are similar to the decrease in diffusion that occurs during axonal degeneration in the sea lamprey.[34] Degeneration of neural structures has also been associated with changes in diffusion throughout the spinal cord.[8] In previous studies, we have reported changes in diffusion within the cervical spinal cord that differ from diffusion in the thoracic injury zone. In the cervical spinal cord, after a T8 injury in rats, we consistently see a reduced MD.[8] Changes remote from injury suggest an increase in cellularity, possibly due to glial proliferation or other pathological process that results in a decrease in MD. The relative localization to the internal capsule is consistent with an overall degradation of corticospinal tracts. Mean diffusivity had the strongest correlation to injury severity; however, each diffusion index may provide unique information into the physiological changes that occur and MD should not be solely relied upon for indication of injury severity.

We observed significant bilateral findings in the internal capsule region of the brain. Others have documented diffusion changes in the internal capsule of the brain following SCI[3, 6]; however, both research groups documented significant unilateral changes in diffusion. The changes reported by both groups differed; Ramu et al. demonstrated an increase in FA (similar to our findings)[3] where Freund et al reported a decrease in FA.[6] While the findings of Freund et al contrast with the current study, it is important to note there could be physiological differences associated with type (complex fracture versus controlled contusion) and time of injury (10 weeks versus multiple years), structural differences due to the injury being in the cervical cord, and differences in species (humans versus rodents). The corticospinal tract descends through both left and right hemispheres into the spinal cord and an injury to the spinal cord that produces sensorimotor dysfunction for all body parts below the lesion would be expected to impact both the left and right internal capsule regions. Sample size may have limited detection of significant bilateral changes in previous

studies. Sample size may also be attributed to the diffusion metrics for the severe group not always being in line with the other group severity levels, as seen in Figure 8. It is important to note that the variation sample groups is high and increasing the sample population could minimize variation and improve the trend in diffusion values as severity increases.

The magnitude of the decrease in mean diffusion in the internal capsule region was correlated with the loss in hindlimb motor function, measured by the BBB scale. Previously our lab has found MD to decrease in the spinal cord in regions extending rostral and caudal to the injury.[35] We have also found that the decrease of mean diffusivity in the cervical segments of the spinal cord correlates to severity of a thoracic injury.[8] Because more severe injuries involve greater numbers of axons, the association of diffusion changes with severity of injury is likely caused by histological changes associated with axon degeneration and/or demyelination.

Injury to one region of the central nervous system results in degeneration of white matter tracts that produce histological changes distant from the injury site itself.[35] The degeneration from a thoracic spinal cord injury elicits tissue structural changes in the cervical dorsal columns,[36-40] that extend into the brainstem.[41] The resulting demyelination and astrocytic response that progresses away from the injury site is localized to the damaged tracts,[42, 43] which would reasonably be associated with the localized path of the corticospinal tract that extends through the pyramids in the brainstem and progresses from the internal capsule region of the brain.[16] Similar changes occur in the opposite direction; cytotoxic inflammation resulting from damage to the motor cortex extends down through the spinal cord in connected axons.[25] Additional tissue structural changes occur as the system recovers. Following a thoracic lesion in the rat, sprouting of descending fibers from the midbrain occurs.[44] These results suggest that damage to one location with the CNS can produce histological changes throughout the white matter tracts of the brain and spinal cord. Diffusivity measurements are sensitive to microstructural changes that occur following CNS damage[2]; thus, it appears that degenerative tissue changes produce the decrease in MD and increase in FA observed in the brainstem and internal capsule in the current study.

Previously documented histological changes in in the brain following SCI were confirmed in the current study.[3,10,11,16] Furthermore, our results indicated a progressive reduction in myelin in the internal capsule as severity of injury increased, based on Luxol fast blue staining. GFAP showed a similar trend with increases in the GFAP expression as injury severity increased. The association of myelin and GFAP with severity of injury was consistent with the correlation between DTI parameters and injury severity. Thus, changes in MD and FA appear to be associated with the decrease in myelin and an increase in astrocytes for the internal capsule region in the brain and the corticospinal tract regions of the brainstem. These results are consistent with the increase in GFAP and lower percentage of myelin basic protein in the internal capsule that have previously been reported to be associated with changes in FA.[3]

Changes in diffusion parameters throughout the brain, including gray matter regions, suggest that the tissue structural changes extend beyond spinal tracts. The changes observed in the gray and white matter were similar, which is consistent with observations of diffusion changes in spinal cord gray and white matter in regions of the remote from the injury site.[8] There have been a limited number of studies that have reported diffusion characteristics in gray matter; however, changes in gray matter diffusion might also be associated with astrocytic activity in response to Wallerian degeneration.[35,40,45]

The high variability of the diffusivity measurements in the brainstem makes it difficult to compare regional differences in the rostrocaudal direction. However, diffusion measurements observed in the brain and spinal cord (in a previous study[8]) allude to less of a decrease in mean diffusivity at more remote locations away from the lesion site. The voxel-based analysis for the t-map comparisons provided a clear representation of the rostrocaudal changes observed in the severity groups. These results suggest that our registration technique allowed for voxel-based analysis, which provided more accurate, less subjective results.

While animal models provide for a more controlled injury and examination of the structural changes that follow, differences in anatomy, pathology, and function could potentially provide different results when the results are translated into a clinical setting. While

studies suggest decreases in MD remote from injury occur following injury for both human and rats,[20,27] changes in the brain following spinal cord injury could differ in the human and rat populations.[3,46] In our study, longer scan times were used to acquire images due to the ex vivo design of the scan study. Although the diffusion metrics resulted in significant changes with respect to injury severity, a thorough investigation with short tolerable scan times in human patients with SCI would better characterize the capabilities of DTI.

Another possible concern for the ex vivo acquired data may be due to the use of formalin-fixed tissue. Sun et al demonstrated similar diffusion rates between live and formalin-fixed mouse brains,[47] Ellingson et al demonstrated similar diffusion values for formalin-fixed spinal cords and neurologically intact spinal cords when compared with numerous studies.[20] However, formalin fixation may still alter water diffusion by reducing the diffusion coefficient magnitude but maintaining anisotropy consistent with in vivo measurements.[20] Formalin-fixed tissue may also affect immunohistochemistry. Prolonged time between tissue fixation and chemical staining may have generated a lower concentration of the anti-body stain adhering to the tissue, thus producing a false negative response.[49]

An improved understanding of the pathophysiological underpinnings of changes in brain DTI after a spinal injury might be obtained from a more detailed histological study. In particular, histological analyses characterizing Wallerian degeneration within the brain following a spinal injury would be particularly interesting. While localization of DTI changes to descending and ascending spinal systems in the current study suggests a localized response, the extent of demyelination, degeneration, and glial proliferation within the brain tracts, similar to analyses near the spinal injury zone would be informative.[28,31] In particular, a histological analysis would provide insight into the cause of the increase in FA, and decrease in RD observed in this study. The histological analysis could also have implications in the rehabilitation of movement after spinal cord injury and could reflect neural plasticity of brain structures in response to spinal injury.

Further insight into the timecourse of morphological and histopathological changes that take place in the brain following a spinal

injury could be obtained from extended in vivo longitudinal DTI measurements in the brain after spinal injury. In vivo scanning of the spinal cord over several weeks in rats and mice, coupled with histological analyses, has provided insight into the histological correlates of DTI changes near the injury site.[28,31] Similarly, scanning the brain at multiple time points could help to determine when diffusion changes in the brain begin and how the demyelinating/degenerating processes in the brain progress after injury. In particular, the time point at which changes in diffusion of the brain occur would provide insight into the secondary injury processes underlying DTI changes in the brain, and might provide insight into interventions aimed at arresting secondary injury, and plasticity of supraspinal neural systems.

In addition to providing measurements at multiple time points, in vivo scanning would provide a more accurate indicator of water diffusion in physiologic conditions. In vivo measurements were originally collected but were not included in this study because the signal to noise ratio (SNR) was too low. The increased time in the ex vivo scans provided higher quality images. Differences in water diffusion between in vivo and ex vivo diffusion images have been documented,[50] with similar results for changes in RD, but less reliable similarities in LD. Although we obtained high resolution images using long scan times by scanning ex vivo, imaging in vivo might provide an imaging model that is more consistent with spinal cord pathophysiology.

In conclusion, we have demonstrated that a traumatic SCI results in diffusion sensitive structural modifications in the brain that are dependent on the severity of injury. Through voxel-based statistical analysis and manually selected ROIs, our results indicated that DTI of the brain is sensitive to varying injury severity following SCI. Diffusion of water in regions associated with tracts that descend into or ascend from the spinal cord was associated with severity of injury. Histological analyses confirmed structural changes in the internal capsule and regions of the corticospinal tract. Results from this study support the hypothesis that DTI of the rat brain is a noninvasive medical imaging technique that is sensitive to injury severity occurring in the spinal cord.

## Acknowledgment

This material is based upon work supported by the Office of Research and Development, Rehabilitation Research and Development Service, Department of Veterans Affairs grant number I01 RX000113. Additional support was provided by the Falk Medical Research Trust and an Advancing a Healthier Wisconsin endowment at the Medical College of Wisconsin. *Author Disclosure Statement:* No competing financial interests exist.

## References

1 Basser PJ, Pierpaoli C. Microstructural and physiological features of tissues elucidated by quantitative-diffusion-tensor MRI. *J Magn Reson B* 1996;111:209–219.

2 Schwartz ED, Hackney DB. Diffusion-weighted MRI and the evaluation of spinal cord axonal integrity following injury and treatment. *Exp Neurol* 2003;184:570–589.

3 Ramu J, Herrera J, Grill R, Bockhorst T, Narayana P. Brain fiber tract plasticity in experimental spinal cord injury: diffusion tensor imaging. *Exp Neurol* 2008;212:100–107.

4 Wrigley PJ, Gustin SM, Macey PM, et al. Anatomical changes in human motor cortex and motor pathways following complete thoracic spinal cord injury. *Cereb Cortex* 2009;19:224–232.

5 Gustin SM, Wrigley PJ, Siddall PJ, Henderson L. Brain anatomy changes associated with persistent neuropathic pain following spinal cord injury. *Cereb Cortex* 2010;20:1409–1419.

6 Freund P, Schneider T, Nagy Z, et al. Degeneration of the injured cervical cord is associated with remote changes in corticospinal tract integrity and upper limb impairment. *PloS One* 2012;7:1–7.

7 Basso DM, Beattie MS, Bresnahan JC. A sensitive and reliable locomotor rating scale for open field testing in rats. *J Neurotrauma* 1995;12:1–21.

8 Jirjis MB, Kurpad SN, Schmit BD. Ex vivo diffusion tensor imaging of varying severity spinal cord injury in rats. *J Neurotrauma* 2013;30:1577–1586.

9 Zhang H, Yushkevich PA, Alexander DC, Gee JC. Deformable registration of diffusion tensor MR images with explicit orientation optimization. *Med Image Anal* 2006;10:764–785.

10 Krassioukov AV, Fehlings MG. Effect of graded spinal cord compression on cardiovascular neurons in the rostro-ventro-lateral medulla. *Neuroscience* 1999; 88:959–973.

11 Endo T, Spenger C, Tominaga T, Brene S, Olson L. Cortical sensory map rearrangement of spinal cord injury: fMRI responses linked to Nogo signalling. *Brain* 2007;130:2951–2961.
12 Kluver H, Barrera E. A method for the combined staining of cells and fibers in the nervous system. *J Neuropathol Exp Neurol* 1953;12:400–403.
13 Ashburner J, Friston KJ. Voxel-based morphometry--the methods. *Neuroimage* 200;11:805–821.
14 Paxinos G, Watson C. *The rat brain in stereotaxic coordinates.* Burlington: Elsevier Academic Press; 2005. 456 p.
15 Cohen J. *Statistical power analysis for the behavioral sciences.* New York: Routledge; 1988. 590 p.
16 Hamano K, Iwasaki N, Takeya T, Takita H. A quantitative analysis of rat central nervous system myelination using the immunohistochemical method for MBP. *Brain Res Dev Brain Res* 1996;93:18–22.
17 Mac Donald CL, Dikranian K, Bayly P, Holtzman D, Brody D. Diffusion tensor imaging reliably detects experimental traumatic axonal injury and indicates approximate time of injury. *J Neurosci* 2007;27:11869–11876.
18 Budde MD, Janes L, Gold E, Turtzo LC, Frank J. The contribution of gliosis to diffusion tensor anisotropy and tractography following traumatic brain injury: validation in the rat using Fourier analysis of stained tissue sections. *Brain* 2011;134:2248–2260.
19 Kakulas BA. Neuropathology: the foundation for new treatments in spinal cord injury. *Spinal Cord* 2004;42:549–563.
20 Ellingson BM, Kurpad SN, Schmit BD. Ex vivo diffusion tensor imaging and quantitative tractography of the rat spinal cord during long-term recovery from moderate spinal contusion. *J Magn Reson Imaging* 2008;28:1068–1079.
21 Schwartz ED, Chin CH, Shumsky, JS, et al. Apparent diffusion coefficients in spinal cord transplants and surrounding white matter correlate with degree of axonal dieback after injury in rats. *AJNR Am J Neuroradiol* 2005;26:7–18.
22 Koshinaga M, Whittemore SR. The temporal and spatial activation of microglia in fiber tracts undergoing anterograde and retrograde degeneration following spinal cord lesion. *J Neurotrauma* 1995;12:209–222.
23 Moisse K, Welch I, Hill T, Volkening K, Strong M. Transient middle cerebral artery occlusion induces microglial priming in the lumbar spinal cord: a novel model of neuroinflammation. *J Neuroinflammation* 2008;5:29–38.
24 Shi F, Zhu H, Yang S, et al. Glial response and myelin clearance in areas of wallerian degeneration after spinal cord hemisection in the monkey *Macaca fascicularis. J Neurotrauma* 2009;26:2083–2096.

25 Weishaupt N, Silasi G, Colbourne F, Fouad K. Secondary damage in the spinal cord after motor cortex injury in rats. *J Neurotrauma* 2010; 27:1387–1397.

26 Gris D, Hamilton EF, Weaver LC. The systemic inflammatory response after spinal cord injury damages lungs and kidneys. *Exp Neurol* 2008;211:259–270.

27 Ellingson BM, Ulmer JL, Kurpad SN, Schmit BD. Diffusion tensor MR imaging in chronic spinal cord injury. *AJNR Am J Neuroradiol* 2008;29:1976–1982.

28 Kim JH, Loy DN, Liang HF, Trinkaus K, Schmidt RE, Song SK. Noninvasive diffusion tensor imaging of evolving white matter pathology in a mouse model of acute spinal cord injury. *Magn Reson Med* 2007;58:253–260.

29 Budde MD, Kim JH, Liang HF, et al. Toward accurate diagnosis of white matter pathology using diffusion tensor imaging. *Magn Reson Med* 2007;57:688–695.

30 Budde MD, Xie M, Cross AH, Song SK. Axial diffusivity is the primary correlate of axonal injury in the experimental autoimmune encephalomyelitis spinal cord: a quantitative pixelwise analysis. *J Neurosci* 2009;29:2805–2813.

31 Brennan FH, Cowin GJ, Kurniawan ND, Ruitenberg MJ. Longitudinal assessment of white matter pathology in the injured mouse spinal cord through ultra-high field (16.4 T) in vivo diffusion tensor imaging. *Neuroimage* 2013;82:574–585.

32 Song SK, Sun SW, Ramsbottom MJ, Chang C, Russell J, Cross AH. Dysmyelination revealed through MRI as increased radial (but unchanged axial) diffusion of water. *Neuroimage* 2002;17:1429–1436.

33 Song SK, Yoshino J, Le TQ, et al. Demyelination increases radial diffusivity in corpus callosum of mouse brain. *Neuroimage* 2005;15:132–140.

34 Takahashi M, Hackney D, Zhang G, et al. Magnetic resonance microimaging of intraxonal water diffusion in live excised lamprey spinal cord. *Proc Natl Acad Sci U S A* 2002;99:16192–16196.

35 Ellingson B, Schmit B, Kurpad S. Lesion growth and deggeneration patterns measured using diffusion tensor 9.4-T magnetic resonance imaging in rat spinal cord injury. *J Neurosurg Spine* 2010;13:181–192.

36 Griffin JW, George R, Lobato C, Tyor WR, Yan LC, Glass GD. Macrophage responses and myelin clearance during Wallerian degeneration: relevance to immune-mediated demyelination. *J Neuroimmunol* 1992;40:153–165.

37 Avellino AM, Hart D, Dailey AT, MacKinnon M, Ellegala D, Kliot M. Differential macrophage responses in the peripheral and central nervous system during wallerian degeneration of axons. *Exp Neurol* 1995;136:183–198.

38 Schwab ME. Repairing the injured spinal cord. *Science* 2002;295:1029–1031.
39 Buss A, Schwab ME. Sequential loss of myelin proteins during Wallerian degeneration in the rat spinal cord. *Glia* 2003;42:424–432.
40 Buss A, Brook GA, Kakulas B, et al. Gradual loss of myelin and formation of an astrocytic scar during Wallerian degeneration in the human spinal cord. *Brain* 2004;127:34–44.
41 Ito T, Oyanagi K, Wakabayashi K, Ikuta F. Traumatic spinal cord injury: a neuropathological study on the longitudinal spreading of the lesions. *Acta Neuropathol* 1996;93:13.
42 Konomi T, Fujiyoshi K, Hikishima K, et al. Conditions for quantitative evaluation of injured spinal cord by in vivo diffusion tensor imaging and tractography: preclinical longitudinal study in common marmosets. *Neuroimage* 2012;63:1841–1853.
43 Deo AA, Grill RJ, Hasan KM, Narayana PA. In vivo serial diffusion tensor imaging of experimental spinal cord injury. *J Neurosci Res* 2006;83:801–810.
44 Raineteau O, Schwab ME. Plasticity of motor systems after incomplete spinal cord injury. *Nat Rev Neurosci* 2001;2:263–273.
45 Ford J, Hackney D, Alsop D, et al. MRI characterization of diffusion coefficients in a rat spinal cord injury model. *Magn Reson Med* 1994;31:488–494.
46 Freund P, Schneider T, Nagy Z, et al. Axonal integrity predicts cortical reorganisation following cervical injury. *J Neurol Neurosurg Psychiatry* 2012;83:629–637.
47 Sun SW, Neil JJ, Song SK. Relative indices of water diffusion anisotropy are equivalent to live and formalin-fixed mouse brains. *Magn Reson Med* 2003;50:743–748.
48 Sun SW, Neil JJ, Liang HF, Schmidt RE, Hsu Cy, Song SK. Formalin fixation alters water diffusion coefficient magnitutde but not anisotropy in infarcted brain. *Magn Reson Med* 2005;53:1447–1451.
49 Fleming JC, Norenberg MD, Ramsay DA, et al. The cellular inflammatory response in human spinal cords after injury. *Brain* 2006;129:3249–3269.
50 Sun SW, Liang HF, Le TQ, Armstrong RC, Cross AH, Song SK. Differential sensitivity of in vivo and ex vivo diffusion tensor imaging to evolving optic nerve injury in mice with retinal ischemia. *Neuroimage* 2006;32:1195–1204.

**Table 1.** BBB Scores (Mean ± Standard Deviation)

| | **1 Day post injury** | **70 Days post injury** |
|---|---|---|
| Control | 14.8±6.8 | 19.1±2.4 |
| Mild | 3.0±2.8 | 15.3±2.4 |
| Moderate | 2.3±4.4 | 13.1±4.0 |
| Severe | 0±0 | 6.3±3.9 |

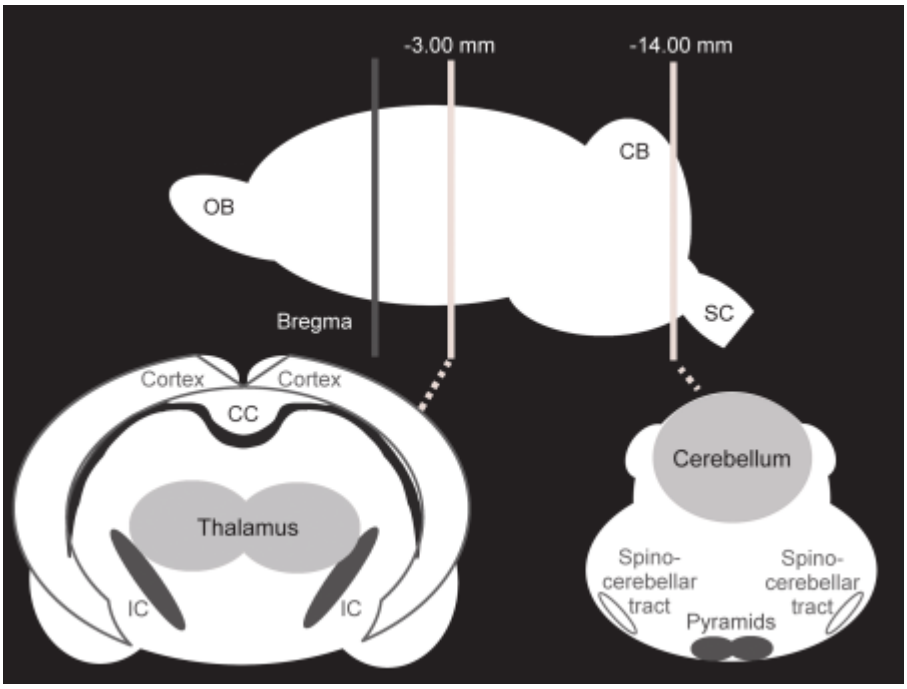


**Figure 1.** Example slice locations of the internal capsule and brainstem. The brain image containing the internal capsule was taken −3.00 mm from bregma and the brainstem slice was taken −14.00 mm from bregma. Abbreviated regions are as follows: olfactory bulbs (OB), cerebellum (CB), spinal cord (SC), corpus collosum (CC), and the internal capsule (IC).

*Journal of Magnetic Resonance Imaging*, Vol 43, No. 1 (January 2016): pg. 63-74. DOI. 

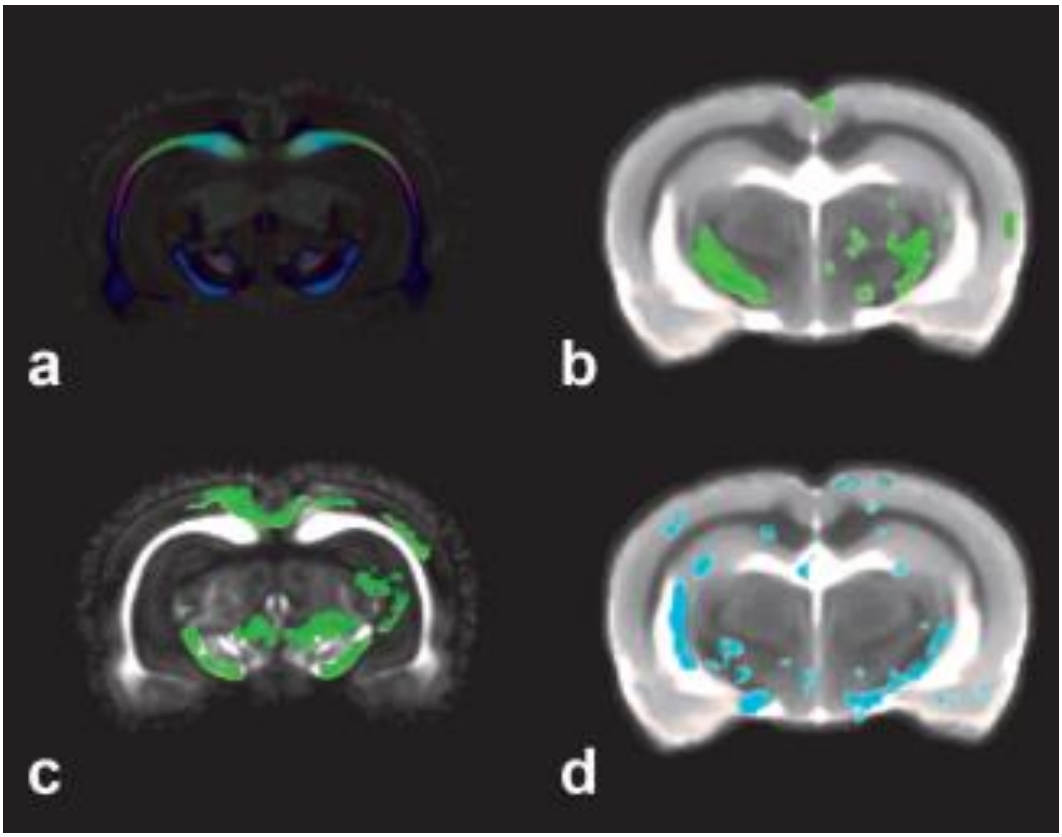


**Figure 2.** A typical RGB map (**a**) demonstrates the rostral to caudal fiber orientation with blue voxels, the green voxels represent fiber orientations in the ventral/dorsal direction, and the red fiber orientation is in the medial/lateral direction. The F-map for mean diffusivity (MD) (**b**), fractional anisotropy (FA) (**c**), and voxel wise (**d**) correlation map between MD and Basso, Beattie, and Bresnahan (BBB) scoring are also shown. Significant differences in variance of the severity groups are identified by green labels ($P < 0.05$) for both MD and FA. Correlation on a voxel by voxel basis between rat MD value and average hindlimb motor score is presented with stronger correlated values ($r^2 > 0.55$) identified in blue. Sections shown are located roughly 3.0 mm posterior to the bregma. Underlay for FA differences (c) and MD differences (b,d) is the sham group for respective indices overlaid onto each other.

*Journal of Magnetic Resonance Imaging*, Vol 43, No. 1 (January 2016): pg. 63-74. DOI. 

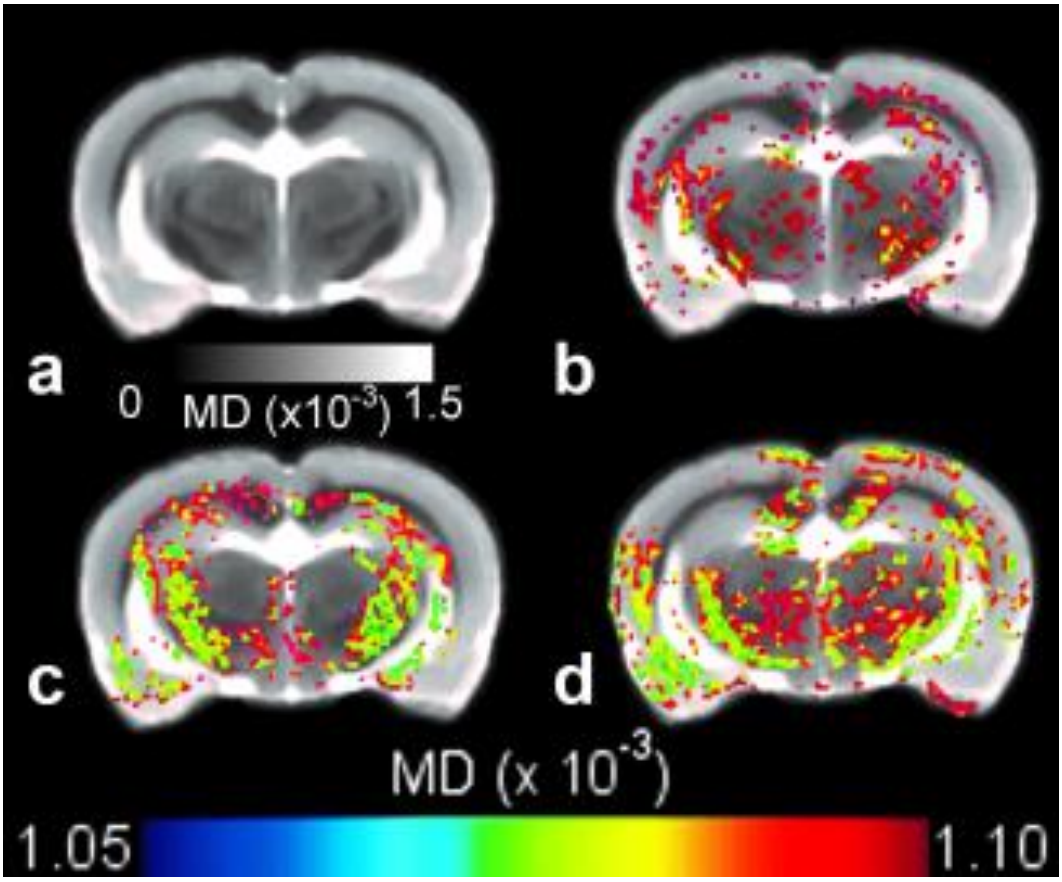


**Figure 3.** Average mean diffusivity (MD) for the sham group (**a**) and the differences (t-maps) between the sham brain and the brains from the mildly (**b**), moderately (**c**), and severely (**d**) injured rats. Sections were taken roughly 3.0 mm posterior to the bregma. Colorized voxels indicate significant differences in variance between the severity groups occurred for mean diffusivity ($P < 0.05$). The associated color index at each significant voxel depicts average MD value for the mildly (b), moderately (c), and severely (d) groups. Underlay for the images is the Mean Diffusivity of each specimen from the sham group overlaid onto each other.

*Journal of Magnetic Resonance Imaging*, Vol 43, No. 1 (January 2016): pg. 63-74. DOI. 

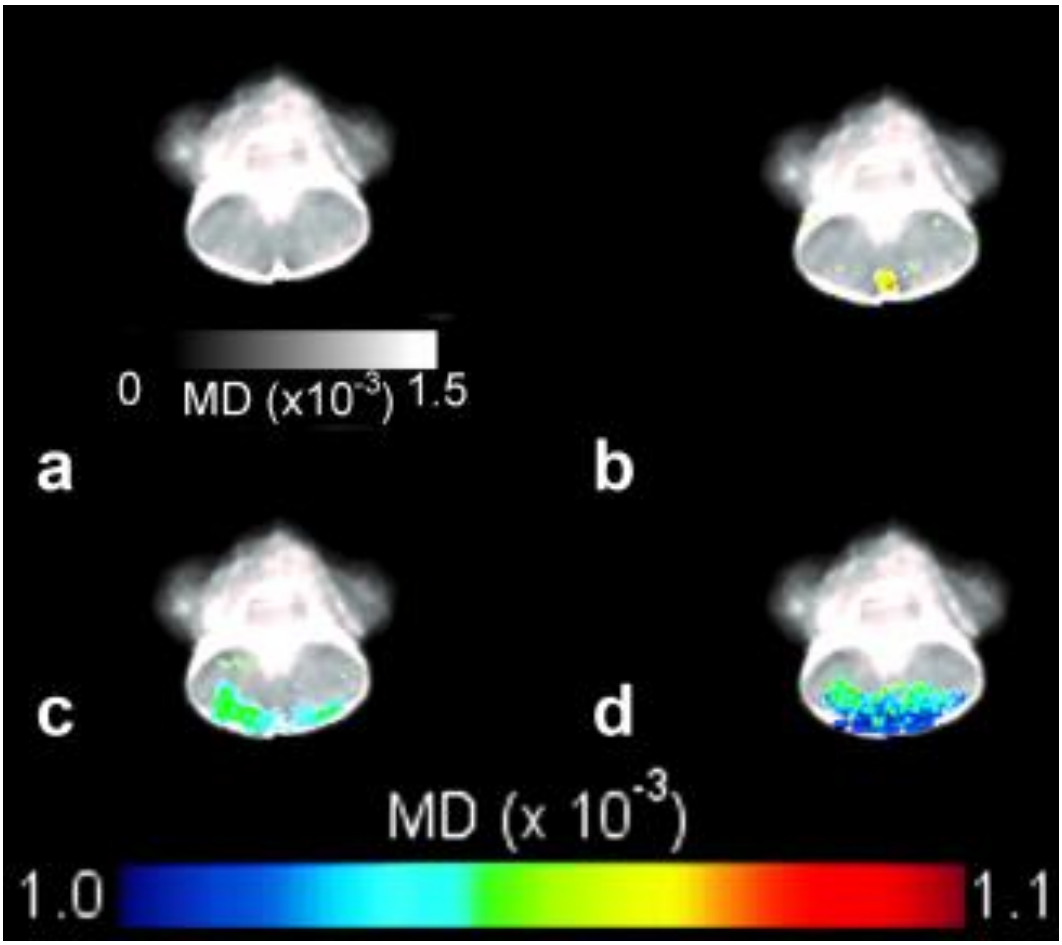


**Figure 4.** Average fractional anisotropy (FA) for the sham group (**a**) and the differences (t-maps) between the sham brain and the brains from the mildly (**b**), moderately (**c**), and severely (**d**) injured rats. Sections were taken roughly 3.0 mm posterior to the bregma. Voxels that contain color represent locations where significant differences in variance between the severity groups occurred for fractional anisotropy ($P < 0.05$). Color index at each significant voxel depicts average FA value for the mild (b), moderate (c), and severe (d) groups. Underlay for the images is the fractional anisotropy of each specimen from the sham group overlaid onto each other.

*Journal of Magnetic Resonance Imaging*, Vol 43, No. 1 (January 2016): pg. 63-74. DOI. 

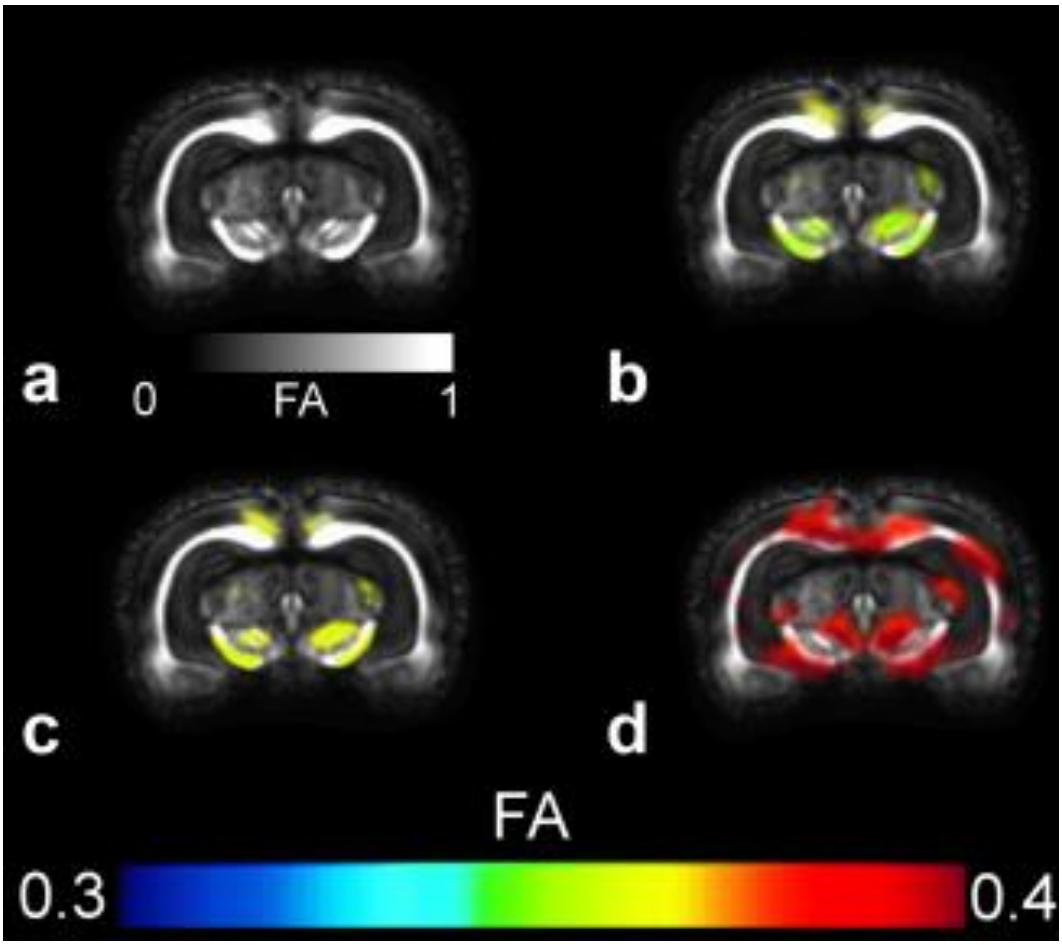


**Figure 5.** Average mean diffusivity (MD) for the sham group (**a**) and the differences (t-maps) between the sham brainstem and the brainstems from the mildly (**b**), moderately (**c**), and severely (**d**) injured rats. Sections were taken roughly 14.0 mm posterior to the bregma. Colorized voxels indicate significant differences in variance between the severity groups occurred for mean diffusivity ($P < 0.05$). The associated color index at each significant voxel depicts average MD value for the mild (b), moderate (c), and severe (d) groups. Underlay for the images is the Mean Diffusivity of each specimen from the sham group overlaid onto each other.

*Journal of Magnetic Resonance Imaging*, Vol 43, No. 1 (January 2016): pg. 63-74. DOI. 

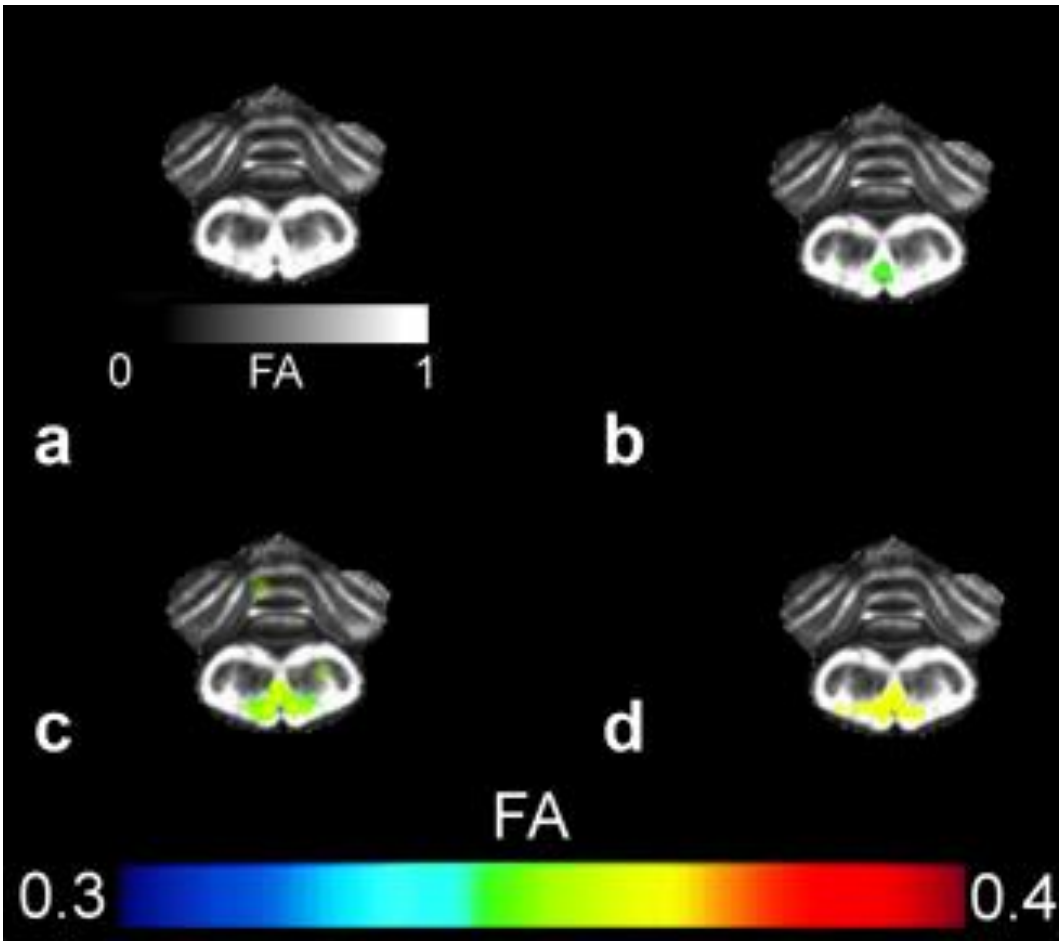


**Figure 6.** Average fractional anisotropy (FA) for the sham group (**a**) and the differences (t-maps) between the sham brainstem and the brainstems from the mildly (**b**), moderately (**c**), and severely (**d**) injured rats. Sections were taken roughly 14.0 mm posterior to the bregma. Voxels that contain color represent locations where significant differences in variance between the severity groups occurred for fractional anisotropy ($P < 0.05$). Color index at each significant voxel depicts average FA value for the mild (b), moderate (c), and severe (d) groups. Underlay for the images is the fractional anisotropy of each specimen from the sham group overlaid onto each other.

*Journal of Magnetic Resonance Imaging*, Vol 43, No. 1 (January 2016): pg. 63-74. DOI. 

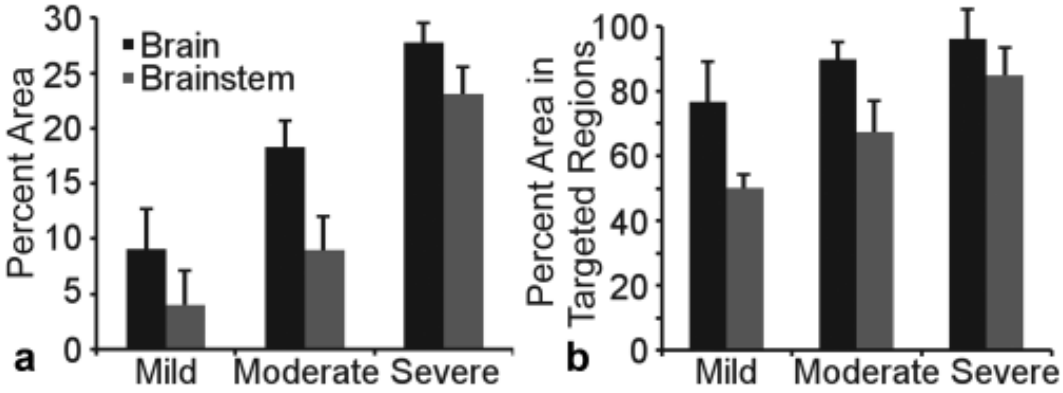


**Figure 7.** Percent volume of significant differences in the brainstem and internal capsule was calculated for the mild, moderate, and severe groups based on measurements of mean diffusivity (MD) (**a**). Significant differences ($P < 0.05$) in voxels occurred when the MD for the selected injury group was different from the control group. Percent of volume that is attributed to either the internal capsule or the pyramidal tracts was determined by normalizing to the entire volume of the region of interest (**b**). Percent volume of significant difference in MD for the internal capsule and pyramid locations increased with severity.

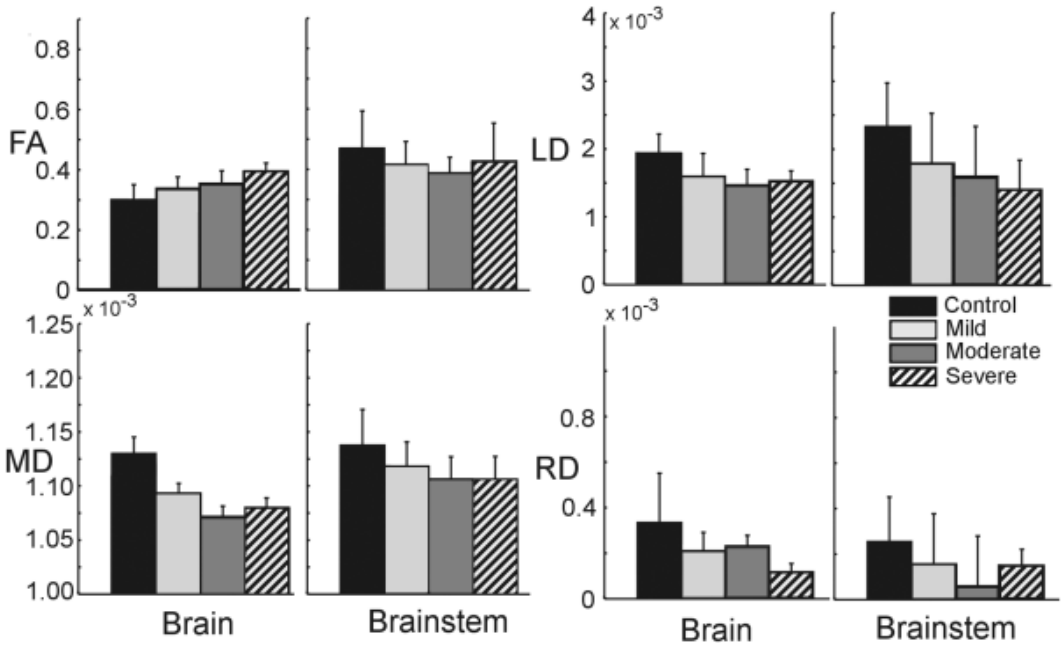


**Figure 8.** Diffusivity measurements for brain and brainstem. Manual region of interest selections for the brain and brainstem were completed for fractional anisotropy (FA), mean diffusivity (MD), radial diffusivity (RD), and axial diffusivity (LD). Error bars indicate standard deviation.

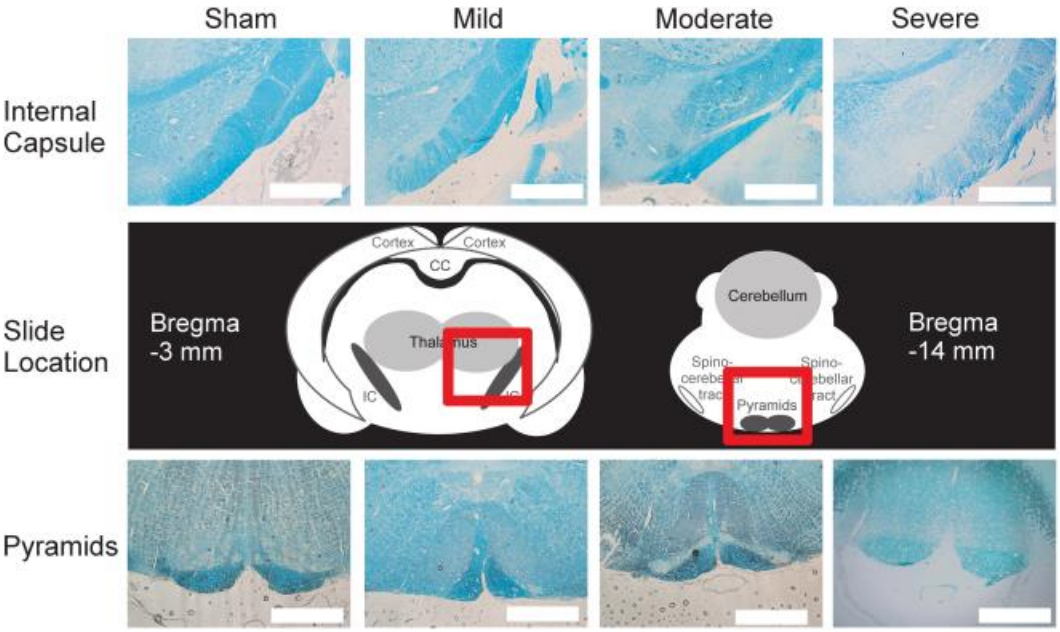


**Figure 9.** Histological examples of un-injured versus injured (left to right) Luxol fast blue stain for myelin in the internal capsule (top row) and the pyramids (bottom row). There is less staining in the white matter as the severity of injury increased which is more evident in the pyramid location in the brainstem.

*Journal of Magnetic Resonance Imaging*, Vol 43, No. 1 (January 2016): pg. 63-74. DOI. 

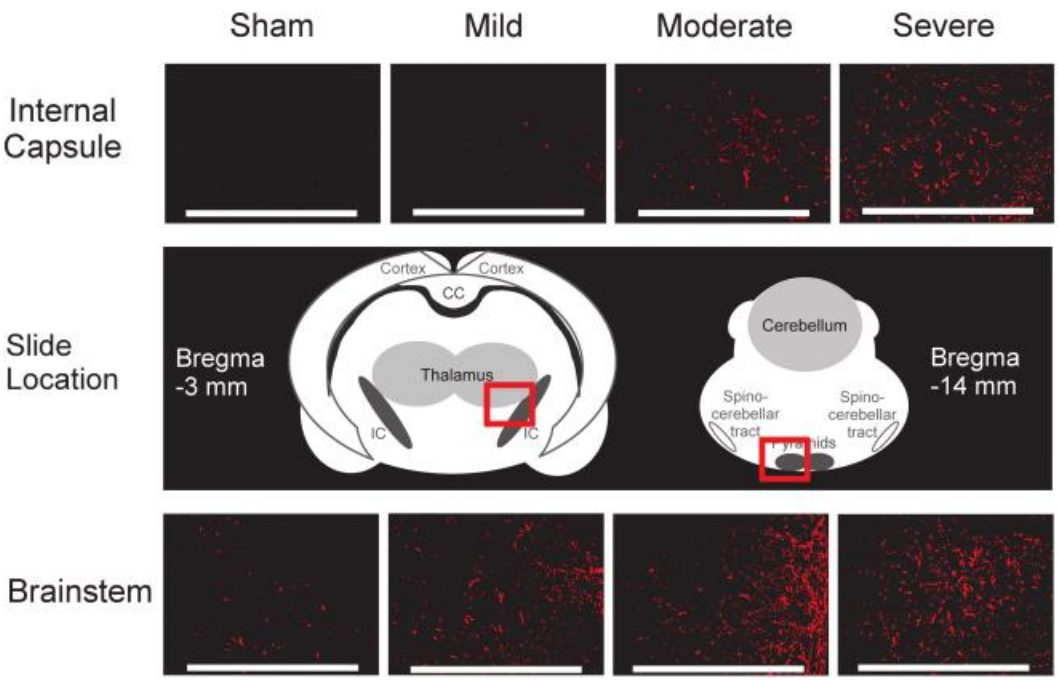


**Figure 10.** Representative glial fibrillary acidic protein (GFAP) immunohistochemical stain for sham, mild, moderate, and severe animal brains in the internal capsule (top row) and brainstem (bottom row) regions. Sections sliced approximately 3.0 mm posterior to the bregma. As the severity increases, there is an increase in expression of GFAP.